Fluid mechanics produces conflicting constraints during olfactory navigation of blue crabs, *Callinectes sapidus*

M. J. Weissburg[1,*], C. P. James[2], D. L. Smee[1] and D. R. Webster[2]

[1]*School of Biology, Georgia Institute of Technology, Atlanta, GA 30332-0230, USA* and [2]*School of Civil & Environmental Engineering, Georgia Institute of Technology, Atlanta, GA 30332-0355, USA*

*Author for correspondence (e-mail: marc.weissburg@biology.gatech.edu)

Summary

Foraging blue crabs must respond to fluid forces imposed on their body while acquiring useful chemical signals from turbulent odor plumes. This study examines how blue crabs manage these simultaneous demands. The drag force, and hence the cost of locomotion, experienced by blue crabs is shown to be a function of the body orientation angle relative to the flow. Rather than adopting a fixed orientation that minimizes the drag, blue crabs decrease their relative angle (increase drag) when odor is present in low speed flow, while assuming a drag-minimizing posture under other conditions. The motivation for crabs to adopt an orientation with larger drag appears to relate to their ability to acquire chemical signal information for odor tracking. In particular, when orienting at a smaller angle relative to the flow direction, more concentrated odor filaments arrive at the antennules to mediate upstream movement, allowing a more useful bilateral comparison between the appendage chemosensors to be made. Blue crabs respond to conflicting demands by weighting the degree of drag minimization in proportion to the potential magnitude of the drag cost and the potential benefit of acquiring chemosensory cues. Higher flow velocity magnifies the locomotory cost of a high drag posture, thus in swift flows crabs minimize drag and sacrifice their ability to acquire olfactory cues.

Key words: chemosensation, drag, fluid dynamics, optimal foraging models, predation, sensory systems, olfaction, *Callinectis sapidus*, crab.

Introduction

Aquatic and terrestrial invertebrates, such as arthropods, rely heavily on chemoperception for many tasks. The ability of these animals to locate prey or mates, or flee predators, varies due to flow-induced modification of sensory cues (Weissburg and Zimmer-Faust, 1993; Vickers and Baker, 1994; Mafra-Neto and Cardé, 1998). Animals exposed to weaker or more intermittent stimuli show decreased search efficiency and lower overall response rates to chemical plumes. For instance, blue crabs (*Callinectes sapidus*) in more turbulent conditions in both the lab and field take more circuitous routes to prey and have lower success rates, suggesting that turbulence intensity is a key flow property that modulates chemosensory-mediated guidance (Weissburg and Zimmer-Faust, 1993).

However, the fluid medium transmits forces in addition to sensory signals, and information gathering is not the only activity that can be strongly affected by fluid flow. Hydrodynamic forces may be particularly important in water due to its relatively high density. Consequently, animals moving through aquatic habitats or exposed to strong ambient flows may experience significant forces that hamper stability and impose a cost on locomotion or appendage movement. Adaptive responses that ameliorate the negative consequences of these forces include postural adjustments, changes in gait or modifications of propulsive movements (Vogel, 1994; Fuiman and Batty, 1997; Martinez et al., 1998).

Searching for distant odor sources using chemical cues implies that animals in fluid environments balance the demands of efficient locomotion and chemical signal acquisition concurrently. Evaluating the effects of flow on organisms therefore may require examining how behavioral responses simultaneously affect multiple tasks. By contrast, most studies have examined either the impact of flow on locomotion (e.g. Blake, 1985; Martinez et al., 1998) or, separately, the influence of the flow environment on signal transmission and reception (e.g. Weissburg and Zimmer-Faust, 1993; Moore and Grills, 1999; Finelli et al., 2000).

The present study examines the potentially competing influences of hydrodynamic forces and odor transport to explain blue crab behavioral responses to the simultaneous demands of efficient locomotion and acquisition of sensory cues. Our data suggest that flow creates conflicting constraints between the ability to move efficiently and to acquire chemosensory information necessary for navigation, such that they cannot be simultaneously maximized. Furthermore, the strategy employed by foraging animals is flexible and contingent upon the relative penalty imposed by the flow,

which suggests that animals assess the tradeoffs involved in adopting a particular tactic in a given flow environment.

Materials and methods

Flow environments

Experiments were conducted in the Environmental Fluid Mechanics Laboratory at Georgia Institute of Technology. A 0.38 m-wide freshwater flume was used for the drag measurements because the flow rate in this facility could be easily varied and rapidly measured. Flow visualization and quantification of the odor plume structure using planar laser-induced fluorescence and the electrochemical probe took place in a large freshwater tilting flume (24 m long×1.07 m wide) capable of generating an equilibrium bed boundary layer. The flow speed, U, was $0.05\,\mathrm{m\,s^{-1}}$ and the flow depth, H, was 0.20 m for these measurements. The tilting flume cannot be used with seawater, so behavioral experiments were performed in a separate saltwater facility (10 m long×0.75 m wide) capable of generating the same flow characteristics as the freshwater flume. In addition to matching the flow conditions above, the behavioral experiments were also performed for a flow speed of $0.10\,\mathrm{m\,s^{-1}}$. In each case, the plume was discharged from a round brass nozzle (4.7 mm diameter) located 0.025 m above the flume bed at a velocity that matched the flume velocity (i.e. an iso-kinetic release). The nozzle perturbed the flow negligibly due to a smooth brass faring on the downstream side, which prevented flow separation.

Drag measurements

The drag force on the crab was measured by summing the moments around a pivot point (Fig. 1). As shown in Fig. 1, the crab was supported at a distance of l_1 below the pivot point. The spring at the end of the lever arm was adjusted to establish a horizontal reference position with no flow. A weight (W, 5.89 N) on the horizontal lever arm provided a moment in the opposite sense to that of the drag force. Measuring the location of the weight relative to the pivot (l_2) and equating the sum of moments to zero yielded the drag force (F_D):

$$F_D = \frac{Wl_2}{l_1} - \frac{F_{shaft}l_{shaft}}{l_1}. \tag{1}$$

The drag force on the submerged section of the support shaft, F_{shaft}, operates at a distance l_{shaft} from the pivot point and is calculated from standard drag coefficient tables for round cylinders (e.g. Munson et al., 2002). The crab specimen was located just above the floor of the flume to mimic walking or swimming blue crabs in a benthic boundary layer. Orientation angles (α) are defined relative to the flow; 0° corresponds to the crab facing directly upstream, whereas 90° corresponds to the crab facing directly to the side (see inset of Fig. 2). Drag forces were measured at angles from 0° through 90° in 15° increments for eight flow velocities between $0.328\,\mathrm{m\,s^{-1}}$ and $0.591\,\mathrm{m\,s^{-1}}$ each with a flow depth of 0.20 m. These velocities are at the high end of the relative water speeds that blue crabs
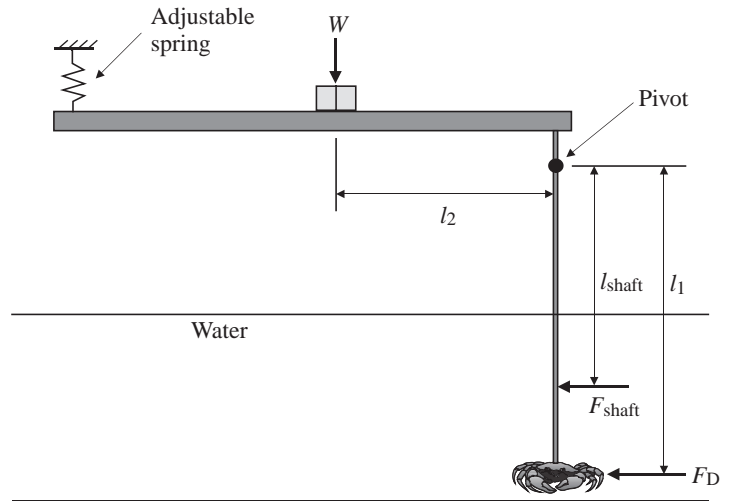

Fig. 1. Schematic of the force balance for the drag measurements. The crab was supported at a distance l_1 below the pivot point. A weight (W) on the horizontal lever arm, at a distance l_2 from the pivot point, provided a moment in the opposite sense to that of the drag force (F_D). F_{shaft} represents the drag force on the submerged section of the support shaft, which is at a distance l_{shaft} below the pivot point.

encounter in tidal channels (i.e. walking speed of $0.1\,\mathrm{m\,s^{-1}}$ in water velocity of $0.03\,\mathrm{m\,s^{-1}}$; Zimmer-Faust et al., 1995). The drag coefficient was found to be constant with Reynolds number (Re) in this range, thus the results can be reliably extended to slightly smaller or larger flow rates.

Five dead crabs (three males and two females) were used for the drag measurements, each with a slightly different size, posture and appendage configuration (Table 1). The legs and claws were fixed with epoxy in positions resembling walking or standing. The frontal projected area of each crab was measured by digitally photographing the animal against a white background and counting the number of pixels within the body shape outline.

The drag coefficient (C_D) is defined as (Munson et al., 2002):

$$C_D = \frac{F_D}{\tfrac{1}{2}\rho U^2 A_{front}}, \tag{2}$$

where ρ is the fluid density and A_{front} is the frontal projected area. It is important to choose the correct representative area for the drag coefficient (e.g. Vogel, 1994). In this case, we

Table 1. *Dimensions of dead crab specimens*

Crab #	Length of carapace (mm)	Distance between tips of lateral spines (mm)	Frontal projected area (mm²)
1	80	162	7 860
2	68	140	6 280
3	75	148	10 620
4	68	145	4 510
5	70	151	4 740

employ the frontal projected area because the streamlines are expected to separate from the crab body, and, hence, the drag force will be dominated by form drag. This is consistent with the uniformity of C_D with varying Re and was confirmed by testing two alternative area definitions, both of which failed to demonstrate dynamic similarity of the C_D data.

Flow visualization

Neutrally buoyant dye was used to observe the plume transport around dead and live crabs. The carapaces of the dead specimens were painted black for visual contrast and were mounted with silicone glue to a white aluminum disk. During the trials, the disk was rotated to produce crab orientations of 0° through 90° at 15° increments. Live crabs were tethered to the disk by snuggly attaching a zip-tie around the crab carapace near the rear legs. Monofilament line was looped through the zip-tie and two small holes in the disk. Thus, the crab was loosely constrained to the disk while allowing normal vertical movements and breathing.

A Kodak digital camera captured the images of the dye plume flowing past the crab. Images were collected from above and from the side for each orientation at two distances from the source: 0.3 m and 1 m. Two dead specimens were employed, one with the front claws tucked near to the carapace, and one with the claws extended in front of the carapace. The live crabs were tested in both freshwater and saltwater flow. Animals tested in the freshwater flume were first acclimated to 5‰ seawater (the salinity of the freshwater flume) over a period of 10 days by reducing the salinity of the holding tanks by 3–5‰ each day. There was no apparent difference in the plume structure near crabs in saltwater *vs* freshwater, so only the latter is reported. In addition to the still images, the live animals were also recorded with a Sony digital camcorder.

Planar laser-induced fluorescence (PLIF)

Planar laser-induced fluorescence measurements provided a quantitative characterization of the odor field around the crab body. The principle of this technique is that fluorescent dye (Rhodamine 6G in this case) absorbs light in the green wavelengths and emits light in the yellow/orange wavelengths. The intensity of the emitted light is proportional to the chemical concentration and the incident light intensity. Thus, after a calibration, the instantaneous concentration distribution in the plane of the laser sheet can be non-intrusively measured.

Webster et al. (in press) previously described the PLIF system in detail. A scanning mirror swept an argon-ion laser beam through the flow in a plane parallel to the channel bed at the elevation of the source nozzle. Images of the emitted light were collected using a Kodak Megaplus ES 1.0 camera over an area of roughly 1 m×1 m. The image capture rate was 10 Hz synchronized with the laser sweep. Data were collected with crabs at three orientations: 0°, 45° and 90°. In each orientation, 6000 consecutive images were collected over a 10-min period, which is sufficient to produce converged mean and S.D. values (Webster and Weissburg, 2001). The *in situ* calibration was performed as described by Webster et al. (in press).

Electrochemical measurements of signal structure

A 10 μm electrochemical sensor, which is sensitive to submicromolar concentrations of dopamine, was used to quantify the signal structure arriving at the chemosensory appendages (Moore et al., 1994). The goal of this series of experiments was to examine whether body orientation changes the character of chemical information arriving at the animal's sensors. Flow visualization indicated that the plume characteristics appeared identical for the live and dead specimens (see Results; Figs 3, 4, 5), which suggests that the breathing current was a mild perturbation to the plume structure. Therefore, data were collected around the appendages of a dead crab specimen located 0.3 m downstream of the odor source for body orientations between 0° and 90°.

Dopamine, prepared in water from the flume at a concentration of 2 mmol l^{-1}, was used as the chemical tracer in the plume. A micromanipulator placed the electrode tip at the level of the dorsal carapace equidistant from the antennules and at the 2nd walking legs on both the right and left sides at a height of 7.5 mm above the substrate for each body orientation. After a 1-min interval to assess the baseline activity, 6.0 min of continuous concentration data were recorded at 5 Hz. The time-average concentration signal statistically converges within this period for this highly intermittent plume (Webster and Weissburg, 2001). The electrode was calibrated immediately prior to the measurements (using a dilution series encompassing the range of concentrations seen in the experiment) and showed a linear response to dopamine concentration ($r^2 > 0.95$).

Behavior

We characterized blue crab search behavior in chemical plumes to examine whether animals alter their body orientation in response to drag and odor presence. Live adult blue crabs, *Callinectes sapidus* L., were purchased from a commercial biological supply company and were housed in saltwater holding tanks adjacent to the flume. Animals were placed in a known starting position 1.5 m downstream of the odor source (9 m from the channel entrance). Attractant odor, created by soaking 7 g l^{-1} of intact, fresh shrimp for 30 min in water taken directly from the flume, was released through the nozzle. Odorless control treatments substituted seawater for shrimp metabolite solutions.

Trials were performed in near darkness (light intensity ≪1 lux) and crabs were not responsive to visual disturbances created by human observers. Red-light-emitting diodes (LEDs), placed dorsally on the left and right sides of each blue crab before the experiment, allowed us to track the animal in the flume. A low-light-sensitive CCD camera mounted approximately 2 m above the working section recorded the behavior. Motion analysis software digitally identified the coordinates of the left and right markers at a rate of 5 Hz to determine body position and orientation. As in the drag, flow visualization and electrochemical measurements, orientation angle is defined relative to the flow. An angle of 0° corresponds to the crab facing directly upstream, whereas 90° corresponds

to the crab facing directly to the side. Not all animals successfully navigated to the source when releasing the shrimp metabolite solution. As we cannot discern whether unsuccessful attempts represent failure to navigate, or a lack of motivation to search, we analyzed only paths of animals that successfully found the source in the presence of odor. Details of these methods may be found in previous publications (Weissburg and Zimmer-Faust, 1993, 1994).

Results

Drag force

Fig. 2 shows the drag coefficient (C_D) data for five crab specimens. The drag coefficient is maximal at the perpendicular (0°) position and decreases with increasing angle, showing roughly a 50% decline between 0° and 90°. Variation in C_D among the specimens at a given angle is attributed largely to small variations of body morphology and appendage position. In these data, A_{front} is held constant (at the value for $\alpha=0°$ reported in Table 1) so the drag force, which is physically relevant to a foraging animal, is proportional to C_D.

Blake (1985) investigated the swimming ability of several decapods, including *Callinectes sapidus*, by measuring the lift and drag forces on the carapace. Although he reached similar
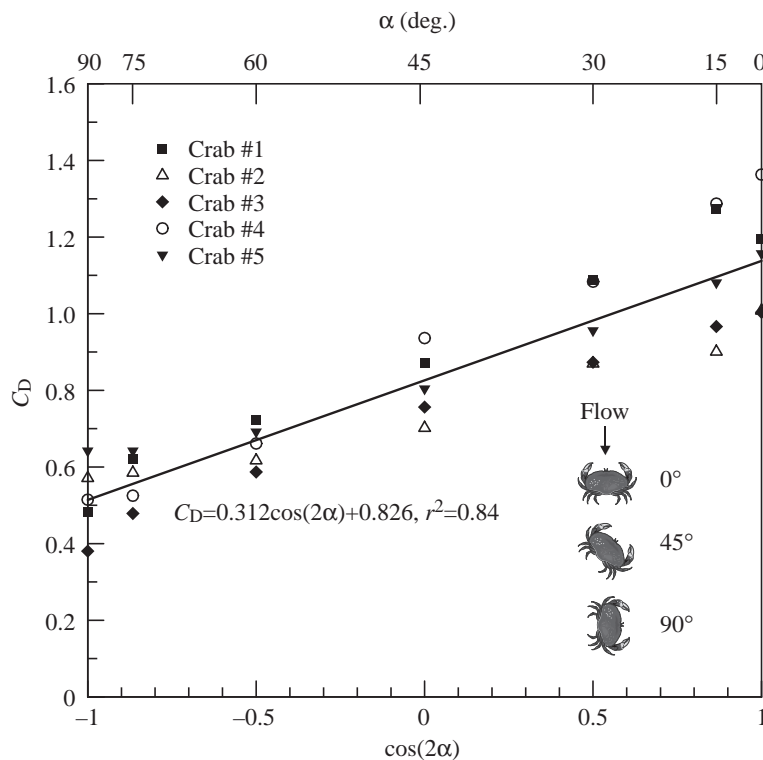
conclusions regarding the orientation angle that minimizes C_D, these experiments cannot be easily compared with the current study. In particular, Blake (1985) performed the measurements on an isolated carapace, cleaned and smoothed with Plasticine, and these surgical modifications substantially alter the measured drag force.

Flow visualization

A flow visualization photograph of the undisturbed plume at a distance of 0.3 meters from the source is shown in Fig. 3A. The plume consists of filaments of high concentration separated by regions of clear fluid, as reported by Webster and Weissburg (2001) and Crimaldi et al. (2002), among others. The chemical signal arriving at a chemosensor, therefore, is highly fluctuating and intermittent. The plume spreads gradually and symmetrically (at least in the time-averaged sense) in the spanwise direction with little meander. The plume also mixes vertically, although the bed appears to constrain the downward growth.

Fig. 3B–D are images of the same plume with the crab at three orientation angles between 0° and 90° (images at increments of 15° for this and another specimen are available in Percy, 2001). The purpose of these images is to gain an appreciation of the plume structure at the chemosensor locations on the claws, legs and antennules. When perpendicular (0°), the presence of the crab body slightly spreads the plume and increases the homogeneity of the plume just upstream of the antennular region, but signals arriving at chemosensors are still visibly intermittent (Fig. 3B). When the body is rotated to 45°, the antennular region is located in the wake of the upstream claw (Fig. 3C). Turbulence intensity is enhanced in the wake of the claw and the dye plume is mixed more thoroughly before arriving at the antennules. Thus, the signal appears more homogeneous at the antennules compared with the undisturbed plume. At 90°, the plume initially contacts the upstream legs and claw and the antennules appear to be exposed to little of the plume structure (Fig. 3D).

Blue crabs have chemosensors on their legs in addition to the sensors on the antennules. The overhead images show that the flow pattern around the crab body draws dye under the carapace where it is highly mixed and spread laterally. These images indicate that the intermittent signal of the undisturbed plume is clearly not maintained at the legs; they appear to be completely inundated with a fairly homogeneous dye field. The plume structure arriving at the legs changes little as orientation angle is increased (Fig. 3D).

The plume also appears more homogeneous in the wake of the crab than it does approaching the animal. The plume expands from approximately one-quarter of the crab body width upstream to nearly the projected width of the crab in the wake (Fig. 3). The increased

Fig. 2. Drag coefficient (C_D) for five crab specimens at orientation angles (α) from 0° to 90°. Based on the expected symmetry of the flow patterns around the crab (i.e. roughly symmetrical left to right and front to back), a functional form of $\cos(2\alpha)$ is assumed for the drag variation with orientation angle. A trend line based on linear regression is shown and yields an r^2 value of 0.84. A third-order polynomial fit with respect to α yielded a similar r^2.

mixing results from the complex flow pattern around the body and increased local turbulent intensity. The wake narrows as the orientation angle increases from 0° to 90°, which is consistent with the decrease in drag coefficient with increasing body angle (Fig. 3; i.e. a narrower wake means a lower momentum deficit and, hence, lower drag force).

Flow visualization trials verify that the breathing current affected the plume minimally, and, hence, flow visualization and measurements around dead crab specimens are a valid indicator of the true flow properties. Indeed, the plume characteristics impinging on the dead crab specimen (Fig. 3C) remain similar for the live specimen oriented at the same angle (Fig. 4); in particular, the plume approaching the animal is filamentous, the wake of the upstream claw homogenized the plume near the antennules, flow under the carapace spreads the plume laterally and the legs are inundated with dye, and the wake of the animal is well mixed and much wider than the upstream plume. Brief excurrent bursts directed downstream or to the side were observed in the freshwater trials and, less frequently, in the saltwater trials. These water jets momentarily add to the turbulence intensity but did not significantly alter the bulk flow pattern.
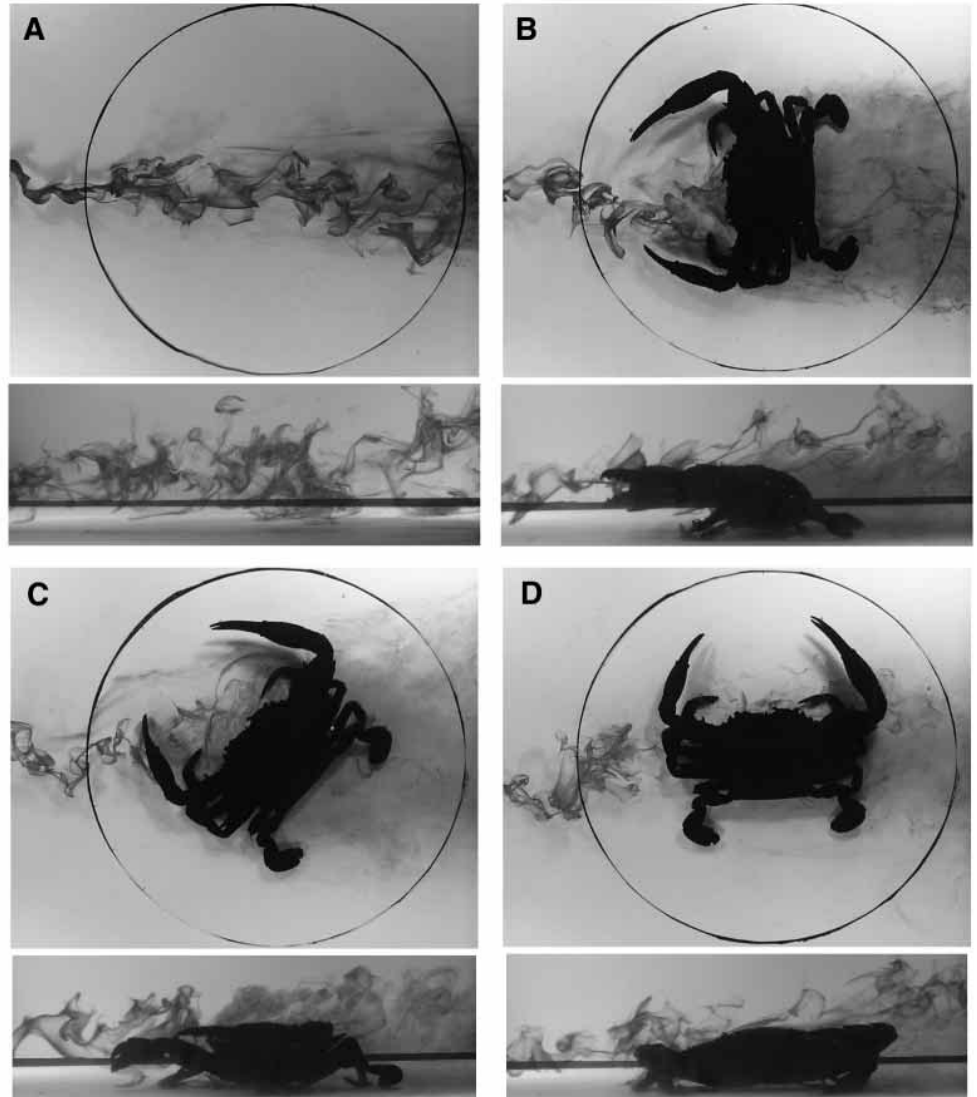

Fig. 3. Flow visualization of odor plumes 0.3 m from the source. Undisturbed plume (A) and a dead crab specimen oriented at 0° (B), 45° (C) and 90° (D). Crab specimen is #2 in Table 1.
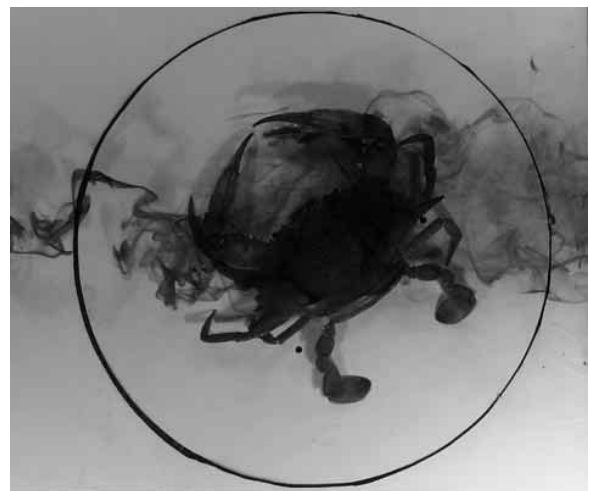
Plume structure around the blue crab

Fig. 5 shows the instantaneous concentration field measured with PLIF in the absence of the crab and with a dead crab specimen at 45°. The center of the crab is at x/H=1.5 (i.e. 0.3 m), and the surrounding flat region corresponds to where the laser sheet is blocked by the crab body. These sample fields again indicate that the crab body negligibly affects the appearance of the plume structure approaching from upstream, whereas peak concentrations in the wake are considerably more dilute due to the presence of the crab body. Additionally, the peaks are spread out over a broader area in the wake as a result of the flow disturbance created by the crab body. These observations support the general impression conveyed in the flow visualization that the major effect of the crab body is in the downstream wake rather than in the plume upstream.

Fig. 4. Flow visualization for a live crab located 0.3 m from the source at an orientation of 45°.
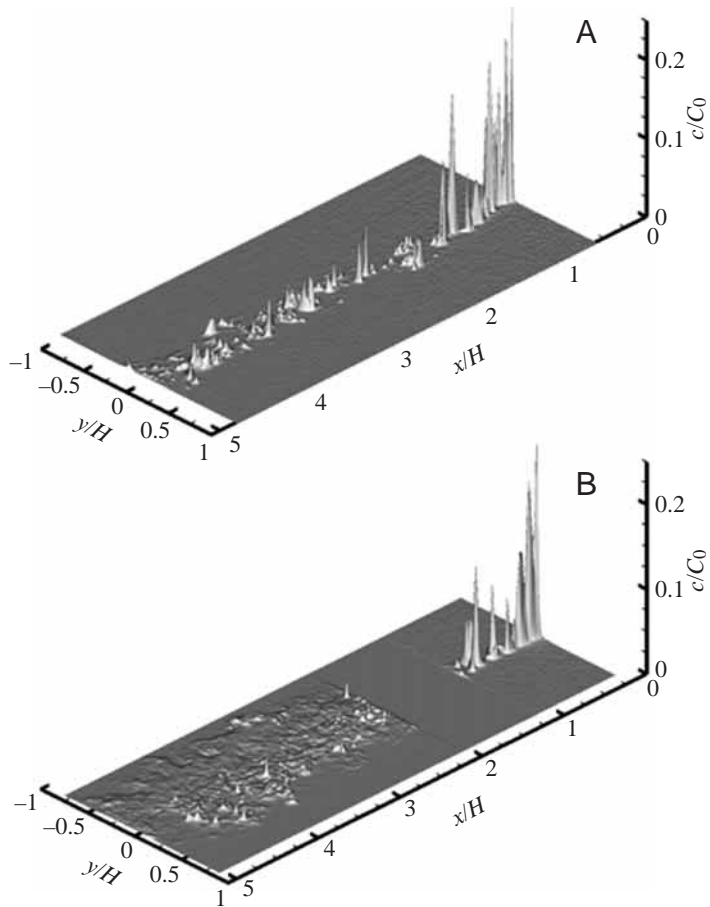
Fig. 5. Instantaneous concentration field for (A) an undisturbed plume and (B) a dead crab specimen oriented at 45°. The filament concentration (c) is normalized by the source concentration C_0, and the streamwise (x) and cross-stream (y) distances are normalized by channel depth H.

Fig. 6. Cross-stream profiles of (A) the filament concentration average ($\bar{c}$) and (B) the standard deviation at x/H=2.5 (see Fig. 5) for three crab orientations. Concentration is normalized by the source concentration C_0, and the cross-stream distance (y) is normalized by the channel depth H.

Fig. 6A shows the time-average concentration profiles at a downstream distance of x/H=2.5 (the center of the crab is at x/H=1.5, thus the profiles are one channel depth behind the crab). The presence of the animal's body dilutes the plume significantly; each profile is lower and wider than the undisturbed profile, which was previously reported in Webster and Weissburg (2001). The 90° orientation produced the narrowest profile and highest peak, whereas the profiles have approximately the same width and concentration peak at orientations of 0° and 45°. As discussed above, the width of the wake is consistent with the drag force measurements. Profiles are basically symmetrical at approximately the center axis at orientations of 0° and 90°, but the 45° orientation shows significant asymmetry resulting from the skewed geometry of the crab body at this angle. The increased homogeneity in the wake of the crab also leads to a smaller standard deviation of the concentration fluctuations (Fig. 6B). The lower S.D. is consistent with the more homogeneous appearance of the plume in the flow visualization trials (Figs 3, 4). The mean and S.D. values are of similar magnitude, thus the concentration is stil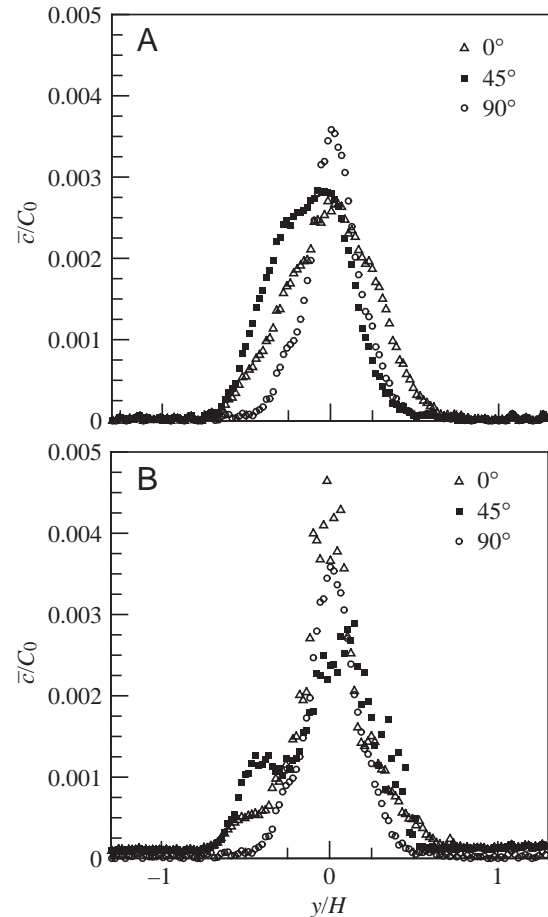l fluctuating greatly around the mean. The S.D. profiles for 0° and 90° have the largest S.D. along the centerline. The peak for the 45° orientation is slightly lower, and the profile shows a second peak at y/H=−0.5, again suggesting an asymmetric wake for this orientation.

Signal structure at the appendages

Data from the electrochemical sensor quantify the chemical signal structure at the chemosensors. Fig. 7 shows the concentration of individual odor filaments (conditionally averaged to include only non-zero readings) and the intermittency factor, defined as the proportion of time that the concentration is above the detectable limit (Chatwin and Sullivan, 1989) as a function of orientation angle. For 0°, the filament concentrations are relatively high because the plume flow path is unobstructed. As the body is rotated towards 90°, the antennules and right (downstream) legs receive signals diluted and mixed by turbulence around the crab's body, and the concentration diminishes. The left (upstream) leg experiences a slight increase in the filament concentration as it moves upstream of the body.

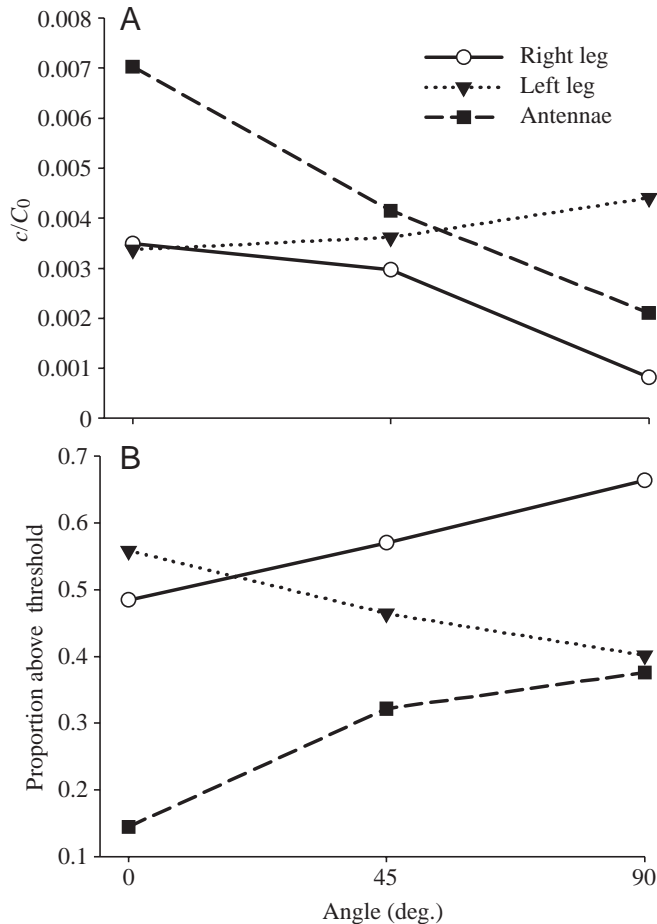The proportion of time that the signal is above the detection

Fig. 7. Chemical signal characteristics near appendages of dead crab specimens as a function of body angle. (A) Average filament concentration (c) normalized by the source concentration C_0 and (B) proportion of samples above the detection threshold (i.e. the intermittency factor). As shown in Fig. 3, the left leg moves upstream as the body is rotated from 0° to 90°.
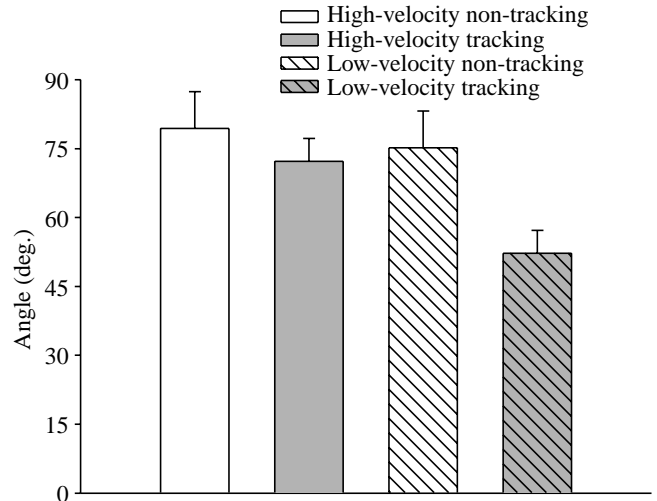

Fig. 8. Mean body angle for crabs in different flow (high- or low-velocity) and odor (tracking or non-tracking) conditions. Graph shows mean path angle for crabs in each treatment group ± 95% confidence limit. The measure of angular dispersion, r (the mean vector length), is 0.98, 0.98, 0.99 and 0.99 for high-velocity non-tracking, high-velocity tracking, low-velocity non-tracking and low-velocity tracking, respectively. Higher values indicate less variation, and the statistic has a maximum value of 1. The difference between mean angles of tracking *vs* non-tracking groups is significant only for the low-velocity flow (Watson–Wheeler test; $F_{1,21}$=92.24, $P\ll0.001$). The confidence limit is derived from r (Batschelet, 1981). Sample sizes consist of 9, 10, 8 and 14 paths for high-velocity non-tracking, high-velocity tracking, low-velocity non-tracking and low-velocity tracking, respectively.

limit is also affected by body angle. With increased orientation angle, the body becomes a significant flow obstruction for the downstream legs, resulting in more-frequent, lower concentration filaments at the antennules and right (downstream) leg. Signal constancy at the antennules and right (downstream) leg therefore increases as the body is rotated towards 90° and decreases at the left leg.

Body orientation behavior

Crabs vary their angular orientation relative to the flow direction depending on both the flow velocity and odor treatment (Fig. 8). Crabs orient their body at an angle nearly parallel (approximately 75°) to the flow except in low flow with odor present, which results in a smaller mean body orientation angle (approximately 52°). Odor presence has a significant effect on body angle for crabs in low, but not high, flow. The distribution of orientation angles during locomotion also varies with odor presence and flow speed (Table 2). At high flow, and at low flow without odor, body orientations are

skewed strongly towards high angles. By contrast, animals tracking odor in low flow often assume low angles during search. Regardless of flow speed, tracking animals show an increase in the proportion of low-angle body orientations relative to animals in the absence of odor. The analysis also reveals that rapid movement speeds of animals tracking odor plumes in high flows are correlated with high body angles (r=–0.40, N=941, $P\ll0.001$; cosine transformation applied to angular data); that is, in these conditions animals assume high drag postures only when moving slowly. This correlation is not evident in other groups, possibly because body orientations are strongly skewed towards high values in the absence of odor, and drag minimization is not as important for animals navigating through odor plumes in slower flows.

Discussion

A combined analysis of hydrodynamic forces, odor signal structure and behavior indicates that body orientation in blue crabs affects both drag costs and plume structure. Blue crabs assume specific body angles during movement that depend on both flow and odor conditions and that have consequences for the structure of odor signals arriving at their chemosensory appendages as well as those structures transmitted downstream. The interactions between body orientation, drag

Table 2. *Distribution of body angles from crab paths in different flow and odor conditions*

	Interval (deg.)					
	0–15	15–30	30–45	45–60	60–75	75–90
High-velocity tracking	0.04	0.03	0.04	0.16	0.37	0.36
High-velocity non-tracking	0.0	0.0	0.0	0.0	0.24	0.76
Tracking *vs* non-tracking	0.04	0.03	0.04	0.16	0.14	–0.40
Low velocity tracking	0.10	0.14	0.14	0.15	0.16	0.30
Low velocity non-tracking	0.0	0.0	0.02	0.10	0.29	0.59
Tracking *vs* non-tracking	0.10	0.14	0.12	0.05	–0.13	–0.29

Table gives the proportion of observations that fall into successive 15° intervals, and the difference between the proportions of tracking *vs* non-tracking animals in each flow velocity. The number of observations equals the number of video frames collected from all paths in a given treatment and totals 941, 1143, 941 and 720 for high-velocity tracking, high-velocity non-tracking, low-velocity tracking and low-velocity non-tracking, respectively.

force and plume structure have a variety of implications for foraging energetics and navigational strategies.

Flow perturbations by the blue crab body

Flow visualization and PLIF images of odor plume structure suggest that animals exert a negligible effect upstream, but that enhanced mixing in the turbulent wake significantly altered odor plume structure downstream of the body for all body orientations. The diminished concentration and increased homogeneity in the wake of the crab may inhibit the odor-tracking ability of another downstream predator. This implies a competitive advantage for the first animal that navigates through the plume, but it seems unlikely that animals actively manipulate the signal structure downstream.

Although the body does not significantly alter the plume structure upstream, there is a large influence of the body orientation on the odor signal structure near the chemosensory appendages. The consequences of this effect are discussed more fully below.

Behavioral optimization in foraging blue crabs

Drag increases the cost of locomotion, and many animals have evolved body forms that reduce drag and, therefore, the energy required for propulsion (Vogel, 1994). Decreased drag also promotes stability against overturning, which offers significant advantages for substrate-bound aquatic creatures such as crabs (Martinez et al., 1998; Martinez, 2001). Given the nearly twofold variation in C_D, *Callinectes* can reduce its cost of locomotion substantially by assuming body angles near 90°. Crabs in high and low flow in the absence of odor oriented at angles very near the drag-minimizing posture; the corresponding C_D at 75° is only 10% higher than the smallest measured value.

Although crabs assume body angles with relatively small drag, they rarely adopt a drag-minimizing posture (i.e. 90°) and, in the presence of odor, more frequently assume orientations with higher drag. The mean angle of animals navigating to odor plumes in low flow was 52°, which is approximately midway between drag-minimizing and -maximizing orientations. By orienting at this angle, crabs

increased C_D by nearly 40% relative to the other treatment. A low mean angle was observed in slow flow only when odor was present, suggesting that changes in body orientation were not solely a response to relaxed energetic penalties in slower flows. Rather, there appears to be a tradeoff between drag minimization and tracking ability that encourages animals navigating in odor plumes to assume orientations that do not minimize drag. This tradeoff was evident to a smaller degree in high flows, where animals tracking odors orient at low angles during slow movement when drag costs are potentially smaller.

The propensity of foraging crabs to adopt a higher drag orientation appears to be related to its ability to acquire useful chemosensory cues. Analysis of chemical signals impinging on chemosensory appendages reveals a significant influence of body orientation and illustrates how signals more conducive to odor tracking occur at low body angles. Blue crabs, and perhaps other crustaceans, rely on an up-current response triggered by detecting odor filaments (Weissburg and Zimmer-Faust, 1993; McLeese, 1973). Orienting at low angles brings chemosensors on the antennae and antennules into contact with less-dilute odor signals. As rapid dilution in turbulent odor plumes may quickly render even highly concentrated stimuli below typical detection thresholds for crustacean chemosensors, orientation at low body angles enhances the perception of relevant odors. Plume tracking also utilizes the asymmetry of odor arrival at bilaterally paired sensory appendages such as legs and antennules (Reeder and Ache, 1980; Devine and Atema, 1982; Zimmer-Faust et al., 1995). Animals react to signal contrast between sensors separated in the cross-stream direction by steering towards the more intensely stimulated side, which keeps them close to the main axis of the plume. Larger sensor spans in the transverse direction improve the signal contrast (Webster et al., 2001). Appendages span a larger cross-stream distance at low body angles, whereas at 90° there is minimal transverse separation because paired appendages are aligned with the plume axis. Additionally, chemosensors on the legs experience differences in frequency and intensity of stimulation, as one member of the pair is located in the wake of the body. Thus, the

asymmetric perturbation of the signal at the leg chemosensors further compromises the animal's ability to determine the lateral position relative to the plume centerline.

Although the precise form of the tradeoff behavior is not known, the data indicate that crabs assume a higher drag orientation when searching for an odor source *via* an odor-gated rheotaxis strategy with bilateral comparison. Thus, crabs appear willing to accept a higher drag force, and higher cost of locomotion, in order to acquire useful chemosensory information under some circumstances. The tradeoff has limits, however. For instance, crabs do not orient at 0°, which provides the strongest signal at the antennules and the best contrast between the leg chemosensors but has the disadvantage of dramatically increasing the drag force. Furthermore, minimizing the drag coefficient is particularly important in high flow because the drag force increases in proportion to the square of velocity (equation 2). Thus, crabs appear unwilling to orient with a high drag coefficient in higher speed flows even in the presence of odor.

Constraints on information gathering

Blue crabs increase their cost of locomotion in order to successfully track odor sources, thus increasing the cost of chemical information gathered during foraging. Economic models of consumer behavior do not generally incorporate costs associated with constraints on sensory systems. However, evidence is accumulating that perceptual mechanisms impose costs on foraging energetics and may have a significant impact on behavior (e.g. Barclay and Brigham, 1994; Spaethe et al., 2001). Animals locating or discriminating objects in flow may respond by either tolerating these costs or reducing them at the expense of sensory information. Blue crabs display clear evidence of these tradeoffs, orienting themselves to increase the availability of chemical signals in slow flows but minimizing the cost of drag in high flows. Such tradeoffs may be common in other organisms using olfactory cues in flow. For instance, moths change their body angle when flying in different conditions, becoming more parallel to both the ground and the wind direction as wind velocity increases (Wilmott and Ellington, 1997; Zanen and Cardé, 1999). This behavior minimizes the frontal area to reduce the drag of moths in flight, but places their chemosensors more directly in line with the body. Thus, upstream propagation of fluid disturbances (e.g. bow wakes) may affect chemical signal structure impinging on sense organs close to the body. Whether postural adjustments reducing drag in response to high wind velocity also degrade or change chemical signals impinging on olfactory receptors remains unknown. Spiny lobsters (*Panulirus argus*) reduce the spread of their antennae during locomotion in proportion to increasing flow velocity. Interestingly, they never adopt a spacing that minimizes drag, perhaps because greatly reducing their antennae spread interferes with their ability to acquire sensory input (Bill and Herrnkind, 1976). In general, tradeoffs between costs associated with sensory perception *vs* other behavioral requirements have not been examined in detail. As suggested here, these tradeoffs are liable to be critically important for cost–benefit models of food finding or other resource acquisition behaviors that utilize chemically mediated guidance.

Flow velocities in habitats occupied by benthic animals change both spatially, as a result of variations in the depth or width of inlets and channels, and temporally during tidal cycles. Crabs adjust their foraging strategy in response to the perceived energetic costs and potential benefits of enhanced foraging efficiency for given conditions. This behavioral flexibility indicates that crabs integrate these potential costs and benefits so that they only assume a high drag posture when the costs are low and odor stimuli indicative of a potential energetic reward are present. Foraging models sometimes incorporate tradeoffs between foraging and other activities, such as predator avoidance or reproduction (e.g. Lima and Dill, 1990; Mangel and Ludwig, 1992). The underlying constraint is that time cannot be allocated simultaneously to two activities, so that the energetic cost of lost foraging opportunity is offset by the benefits of increasing time spent performing another task. Nearly all models of foraging tradeoffs are similarly formulated in terms of time allocation. However, this is not an appropriate model for tradeoffs involving conflicting constraints that balance expected energetic penalties during locomotion with energetic gains associated with more-effective odor tracking, because these two activities occur simultaneously. Animals may choose flow habitats based on these cost–benefit functions, and the ability of animals to forage effectively in flow has substantial impacts on community properties (Leonard et al., 1998). Different modeling approaches, as well as further insights on chemical signal transmission and reception, will be necessary to assess tradeoffs between locomotion and chemoperception and how this may translate into patterns of habitat choice and predatory intensity.

Navigational strategies in turbulent plumes

Terrestrial and aquatic arthropods use rapidly acquired cues in highly intermittent turbulent odor plumes to navigate towards an odor source (Weissburg, 2000; Vickers, 2000). This has led to a widely shared opinion that turbulence is the relevant flow property for explaining tracking success, an idea that has been verified using behavioral experiments decoupling turbulence intensity from bulk flow velocity (Weissburg and Zimmer-Faust, 1993). Thus, it is somewhat ironic to discover that flow speed may also impact tracking success by causing behavioral changes that alter signal acquisition ability. Future efforts to understand olfactory processes in flow need to carefully distinguish among physical effects due to changes in signal structure and flow-induced modifications in behavioral and sensory processes that modulate the ability of animals to acquire information from those chemical signals.

References

Barclay, R. M. R. and Brigham, R. M. (1994). Constraints on optimal foraging: a field test of prey discrimination by echolocating insectivorous bats. *Anim. Behav.* **48**, 1013-1021.

Batschelet, E. (1981). *Circular Statistics in Biology*. London: Academic Press.

Bill, R. G. and Herrnkind, W. F. (1976). Drag reduction by formation movement in spiny lobsters. *Science* **193**, 1146-1148.

Blake, R. W. (1985). Crab carapace hydrodynamics. *J. Zool.* **207**, 407-423.

Chatwin, P. C. and Sullivan, P. J. (1989). The intermittency factor of scalars in turbulence. *Phys. Fluids A* **1**, 761-763.

Crimaldi, J. P., Wiley, M. B. and Koseff, J. R. (2002). The relationship between mean and instantaneous structure in turbulent passive scalar plumes. *J. Turbulence* **3**, 1-24.

Devine, D. V. and Atema, J. (1982). Function of chemoreceptor organs in spatial orientation of the lobster, *Homarus americanus*: differences and overlap. *Biol. Bull.* **163**, 144-153.

Finelli, C. M., Pentcheff, N. D., Zimmer, R. K. and Wethey, D. S. (2000). Physical constraints on ecological processes: A field test of odor-mediated foraging. *Ecology* **81**, 784-797.

Fuiman, L. A. and Batty, R. S. (1997). What a drag it is getting cold: portioning the physical and physiological effects of temperature on fish swimming. *J. Exp. Biol.* **200**, 1745-1755.

Leonard, G. H., Levine, J. M., Schmidt, P. R. and Bertness, M. D. (1998). Flow driven variation in intertidal community structure in a Maine estuary. *Ecology* **79**, 1395-1411.

Lima, S. L. and Dill, L. M. (1990). Behavioral decisions under the risk of predation: a review and prospectus. *Can. J. Zool.* **68**, 619-640.

Mafra-Neto, A. and Cardé, R. T. (1998). Rate of realized interception on pheromone pulses in different wind speeds modulates almond moth orientation. *J. Comp. Physiol. A* **182**, 563-572.

Mangel, M. and Ludwig, D. (1992). Definition and evaluation of the fitness of behavioral and developmental programs. *Ann. Rev. Ecol. Syst.* **23**, 507-536.

Martinez, M. M. (2001). Running in the surf: Hydrodynamics of the shore crab *Grapsus tenuicrustatus*. *J. Exp. Biol.* **204**, 3097-3112.

Martinez, M. M., Full, R. J. and Koehl, M. A. R. (1998). Underwater punting by an intertidal crab: a novel gait revealed by the kinematics of pedestrian locomotion in air versus water. *J. Exp. Biol.* **201**, 2609-2623.

McLeese, D. W. (1973). Orientation of lobsters (*Homarus americanus*) to odor. *J. Fish. Res. Board Can.* **30**, 838-840.

Moore, P. A. and Grills, J. L. (1999). Chemical orientation to food by the crayfish *Orconectes rusticus*: influence of hydrodynamics. *Anim. Behav.* **58**, 953-963.

Moore, P. A., Weissburg, M. J., Parrish, J. M., Zimmer-Faust, R. K. and Gerhardt, G. A. (1994). Spatial distribution of odors in simulated benthic boundary layer flows. *J. Chem. Ecol.* **20**, 255-279.

Munson, B. R., Young, D. F. and Okiishi, T. H. (2002). *Fundamentals of Fluid Mechanics*, 4th edn. New York: Wiley.

Percy, C. M. (2001). The influence of fluid mechanics on the orientation behavior of blue crabs. MS Thesis, Georgia Institute of Technology, Atlanta, Georgia.

Reeder, P. B. and Ache, B. W. (1980). Chemotaxis in the Florida spiny lobster, *Panulirus argus*. *Anim. Behav.* **28**, 831-839.

Spaethe, J., Tautz, J. and Chitka, L. (2001). Visual constraints in foraging bumblebees: flower size and color affect search time and flight behavior. *Proc. Natl. Acad. Sci. USA* **98**, 3898-3903.

Vickers, N. J. (2000). Mechanisms of animal navigation in odor plumes. *Biol. Bull.* **198**, 203-212.

Vickers, N. J. and Baker, T. C. (1994). Reiterative responses to single strands of odor promote sustained upwind flight and odor source location by moths. *Proc. Natl. Acad. Sci. USA* **91**, 5756-5760.

Vogel, S. (1994). *Life in Moving Fluids*. Princeton, NJ: Princeton University Press.

Webster, D. R., Rahman, S. and Dasi, L. P. (2001). On the usefulness of bilateral comparison to tracking turbulent chemical odor plumes. *Limnol. Oceanogr.* **46**, 1048-1053.

Webster, D. R., Rahman, S. and Dasi, L. P. (in press). Laser-induced fluorescence measurements of a turbulent plume. *J. Eng. Mechanics.*

Webster, D. R. and Weissburg, M. J. (2001). Chemosensory guidance cues in a turbulent chemical odor plume. *Limnol. Oceanogr.* **46**, 1034-1047.

Weissburg, M. J. (2000). The fluid dynamical context of chemosensory behavior. *Biol. Bull.* **198**, 188-202.

Weissburg, M. J. and Zimmer-Faust, R. K. (1993). Life and death in moving fluids: Hydrodynamic effects on chemosensory-mediated predation. *Ecology* **74**, 1428-1443.

Weissburg, M. J. and Zimmer-Faust, R. K. (1994). Odor plumes and how blue crabs use them in finding prey. *J. Exp. Biol.* **197**, 349-375.

Wilmott, A. P. and Ellington, C. P. (1997). The mechanics of flight in the hawkmoth *Manduca sexta* I. Kinematics of hovering and forward flight. *J. Exp. Biol.* **200**, 2705-2722.

Zanen, P. O. and Cardé, R. T. (1999). Directional control by male gypsy moths of upwind flight along a pheromone plume in three wind speeds. *J. Comp. Physiol. A* **184**, 21-35.

Zimmer-Faust, R. K., Finelli, C. M., Pentcheff, N. D. and Wethey, D. S. (1995). Odor plumes and animal navigation in turbulent water flows: a field study. *Biol. Bull.* **188**, 111-116.